

Electronic Supplementary Information

**Di- and octanuclear dysprosium clusters derived from pyridyl-triazole based ligand: {Dy<sub>2</sub>} showing single-molecule magnet behaviour**

Muhammad Nadeem Akhtar, Xiao-Fen Liao, Yan-Cong Chen, Jun-Liang Liu\*, Ming-Liang Tong\*

MOE Key Laboratory of Bioinorganic and Synthetic Chemistry, School of Chemistry, Sun Yat-Sen University, Guangzhou 510275, P.R. China

**Contents**

**Table S1.** Selected bond lengths and angles for **1**.

**Table S2.** Selected bond lengths and angles for **2**.

**Table S3.** Continuous Shape Measures (CShM) calculations for **1** and **2**.

**Figure S1.** Curie-Weiss law fittings for **1** and **2**.

**Figure S2.** Temperature dependent in-phase ( $\chi_M'$ ) and out-of-phase ( $\chi_M''$ ) ac signal for **2**.

**Figure S3.** Temperature dependent in-phase ( $\chi_M'$ ) and out-of-phase ( $\chi_M''$ ) signal for **1**.

**Figure S4.** Field dependence of in-phase ( $\chi_M'$ ) and out-of-phase ( $\chi_M''$ ) susceptibilities at 4 K under different fields for **1**.

**Figure S5.** Field dependence of the relaxation time at 4 K for **1**.

**Figure S6.** Cole–Cole plot for **1**.

**Figure S7.** The calculated orientations of the ground-state magnetic anisotropy of each local Dy(III) ion for **1** and **2**.

**Table S1.** Selected Bond Lengths ( $\text{\AA}$ ) and Angles ( $^\circ$ ) for **1**.

Dy(1)–O(1) <sup>i</sup>	2.291(4)	Dy(2)–O(3)	2.251(4)
Dy(1)–O(1)	2.318(5)	Dy(2)–O(3) <sup>ii</sup>	2.260(4)
Dy(1)–O(2)	2.440(4)	Dy(2)–O(4)	2.424(4)
Dy(1)–N(5)	2.575(5)	Dy(2)–N(13)	2.555(5)
Dy(1)–N(2)	2.539(5)	Dy(2)–N(10)	2.542(5)
Dy(1)–N(1)	2.577(5)	Dy(2)–N(9)	2.606(5)
Dy(1)–N(8)	2.571(5)	Dy(2)–N(16)	2.590(5)
Dy(1)–Cl(1)	2.7674(13)	Dy(2)–Cl(2)	2.7799(13)
Dy(1)–O(1)–Dy(1)	108.0(2)	Dy(2)–O(3)–Dy(2)	111.22(18)

Symmetry codes: (i) 2-x, 1-y, 1-z(ii) 1-x, 2-y, -z

**Table S2.** Selected Bond Lengths ( $\text{\AA}$ ) and Angles ( $^\circ$ ) for **2**.

Dy(1)–O(1)	2.275(12)	Dy(5)–O(5)	2.282(13)
Dy(1)–O(8)	2.304(14)	Dy(5)–O(4)	2.311(16)
Dy(1)–N(54)	2.464(17)	Dy(5)–N(22)	2.434(18)
Dy(1)–N(2)	2.499(15)	Dy(5)–N(34)	2.485(18)
Dy(1)–N(61)	2.546(16)	Dy(5)–N(29)	2.473(19)
Dy(1)–N(59)	2.546(18)	Dy(5)–N(27)	2.560(18)
Dy(1)–N(1)	2.620(19)	Dy(5)–N(24)	2.634(16)
Dy(1)–N(56)	2.651(15)	Dy(5)–N(33)	2.70(2)
Dy(2)–O(1)	2.278(13)	Dy(6)–O(5)	2.276(15)
Dy(2)–O(2)	2.288(14)	Dy(6)–O(6)	2.309(13)
Dy(2)–N(62)	2.435(15)	Dy(6)–N(30)	2.398(16)
Dy(2)–N(5)	2.465(16)	Dy(6)–N(37)	2.463(18)
Dy(2)–N(10)	2.529(16)	Dy(6)–N(42)	2.536(17)
Dy(2)–N(64)	2.599(17)	Dy(6)–N(32)	2.545(18)
Dy(2)–N(9)	2.631(18)	Dy(6)–N(35)	2.596(18)
Dy(2)–N(3)	2.638(16)	Dy(6)–N(41)	2.607(16)
Dy(3)–O(3)	2.245(13)	Dy(7)–O(7)	2.238(14)
Dy(3)–O(2)	2.354(14)	Dy(7)–O(6)	2.298(13)
Dy(3)–N(6)	2.436(17)	Dy(7)–N(38)	2.404(17)
Dy(3)–N(13)	2.501(18)	Dy(7)–N(50)	2.481(15)
Dy(3)–N(18)	2.513(18)	Dy(7)–N(45)	2.525(16)
Dy(3)–N(11)	2.566(17)	Dy(7)–N(49)	2.56(2)
Dy(3)–N(8)	2.566(17)	Dy(7)–N(43)	2.608(19)
Dy(3)–N(17)	2.62(2)	Dy(7)–N(40)	2.633(15)

Dy(4)–O(4)	2.305(16)	Dy(8)–O(8)	2.266(13)
Dy(4)–O(3)	2.320(13)	Dy(8)–O(7)	2.333(14)
Dy(4)–N(14)	2.405(16)	Dy(8)–N(46)	2.424(14)
Dy(4)–N(21)	2.457(18)	Dy(8)–N(53)	2.492(16)
Dy(4)–N(26)	2.516(17)	Dy(8)–N(58)	2.512(17)
Dy(4)–N(19)	2.556(16)	Dy(8)–N(51)	2.582(17)
Dy(4)–N(25)	2.61(2)	Dy(8)–N(57)	2.612(18)
Dy(4)–N(16)	2.636(19)	Dy(8)–N(48)	2.612(19)
Dy(1)–O(1)–Dy(2)	125.5(6)	Dy(2)–O(2)–Dy(3)	120.2(6)
Dy(3)–O(3)–Dy(4)	122.3(6)	Dy(4)–O(4)–Dy(5)	118.2(7)
Dy(5)–O(5)–Dy(6)	124.0(6)	Dy(6)–O(6)–Dy(7)	121.1(6)
Dy(7)–O(7)–Dy(8)	121.6(6)	Dy(8)–O(8)–Dy(1)	120.3(6)

**Table S3.** Continuous Shape Measures (CShM) calculations for **1** and **2**.<sup>a</sup>

Complex	OP-8	HPY-8	HBPY-8	CU-8	SAPR-8	TDD-8	JGBF-8	JETBPY-8	JBTPR-8	BTPR-8	JSD-8	TT-8	ETBPY-8
<b>1</b>	Dy1	31.042	22.253	16.185	9.364	1.389	1.176	15.523	28.234	3.013	1.951	4.600	10.001
	Dy2	31.515	21.653	16.299	9.285	1.559	1.442	15.830	28.251	3.211	2.103	5.037	9.920
<b>2</b>	Dy1	31.385	20.671	15.556	11.000	1.246	2.012	14.497	27.956	2.630	1.815	4.713	11.718
	Dy2	32.173	20.838	14.566	8.602	1.502	1.491	16.036	28.131	3.455	2.515	5.202	9.154
	Dy3	32.053	20.576	15.175	10.076	1.571	1.617	15.381	29.236	2.814	1.902	4.554	10.900
	Dy4	32.178	20.678	15.240	9.755	1.179	2.032	15.932	29.278	3.089	1.966	5.551	10.321
	Dy5	31.861	19.951	15.571	10.845	1.411	1.867	15.024	28.792	2.791	1.683	4.549	11.525
	Dy6	31.632	20.317	14.877	9.465	1.431	1.626	15.680	28.987	3.038	2.037	5.030	10.082
	Dy7	32.954	21.145	14.968	9.605	1.757	1.466	15.721	29.565	3.065	2.174	4.759	10.271
	Dy8	31.644	20.954	14.828	9.531	1.091	2.256	15.125	28.451	3.004	1.958	5.520	10.141

OP-8 = Octagon; HPY-8 = Heptagonal pyramid; HBPY-8 = Hexagonal bipyramid; CU-8 = Cube; SAPR-8 = Square antiprism; TDD-8 =Triangular dodecahedron; JGBF-8 = Johnson gyrobifastigium

J26; JETBPY-8 = Johnson elongated triangular bipyramid J14; JBTPR-8 = Bi augmented trigonal prism J50; BTPR-8 = Bi augmented trigonal prism; JSD-8 = Snub dipheroid J84; TT-8 = Triakis tetrahedron; ETBPY-8 = Elongated trigonal bipyramide.

<sup>a</sup> (a) S. Alvarez, P. Alemany, D. Casanova, J. Cirera, M. Llunell and D. Avnir, *Coord. Chem. Rev.*, 2005, **249**, 1693; (b) D. Casanova, M. Llunell, P. Alemany and S. Alvarez, *Chem. Eur. J.*, 2005, **11**,

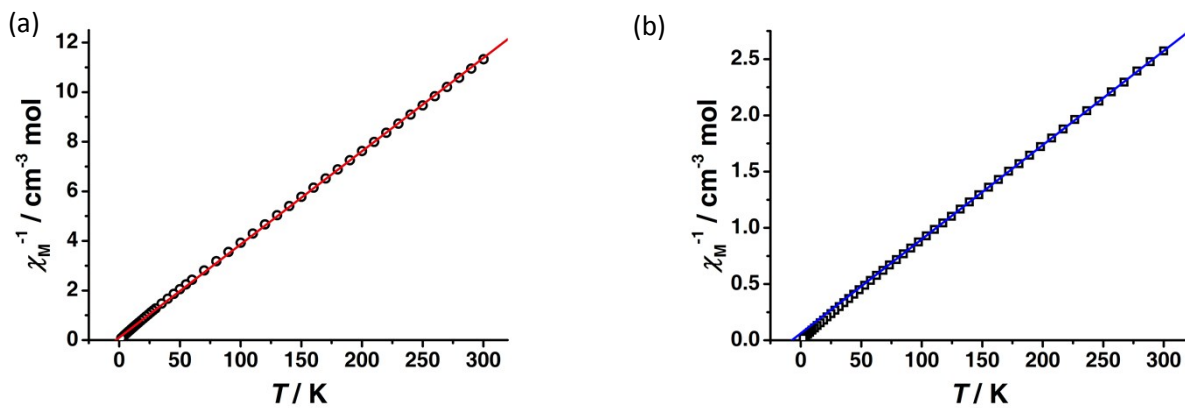


**Figure S1.** Curie-Weiss law fittings for **1** and **2**, giving  $C = 26.6(1) \text{ cm}^3 \text{ K mol}^{-1}$ ,  $\vartheta = -2.6(3) \text{ K}$  for **1** (a), and  $C = 119.4(2) \text{ cm}^3 \text{ K mol}^{-1}$ ,  $\vartheta = -7.3(2) \text{ K}$  for **2** (b).

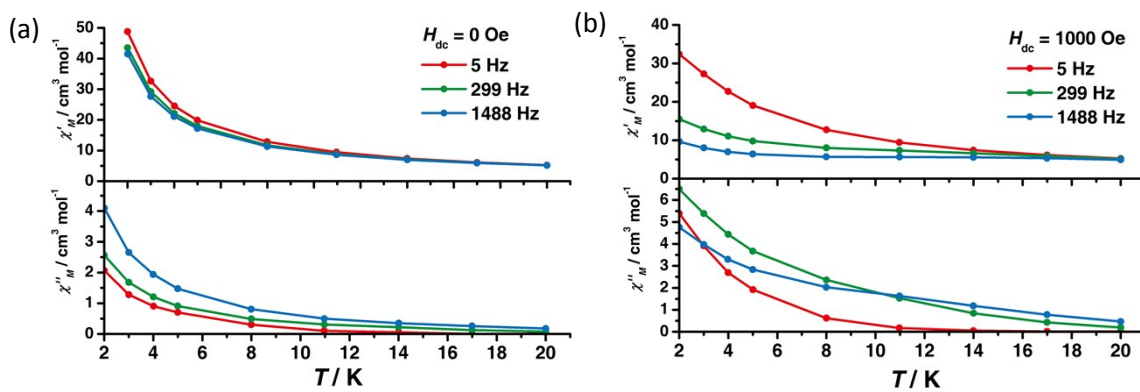


**Figure S2.** Temperature dependent in-phase ( $\chi_M'$ ) and out-of-phase ( $\chi_M''$ ) signal for **2** under zero (a) and 1000 (b) Oe dc field.

The solid lines are guides to the eyes.

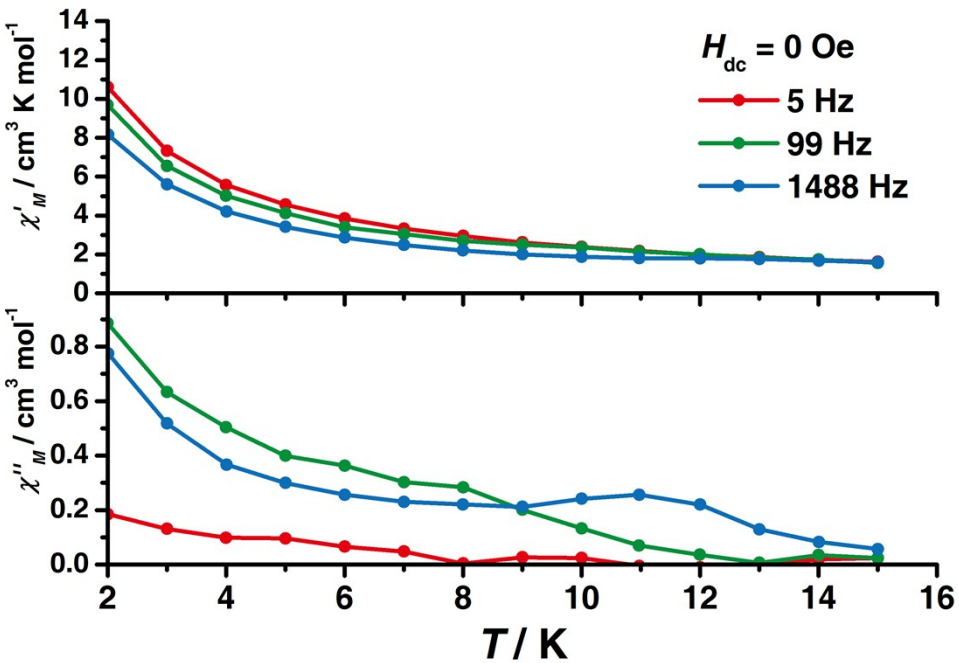


**Figure S3.** Temperature dependent in-phase ( $\chi_M'$ ) and out-of-phase ( $\chi_M''$ ) signal for **1** under zero dc field. The solid lines are guides to the eyes.

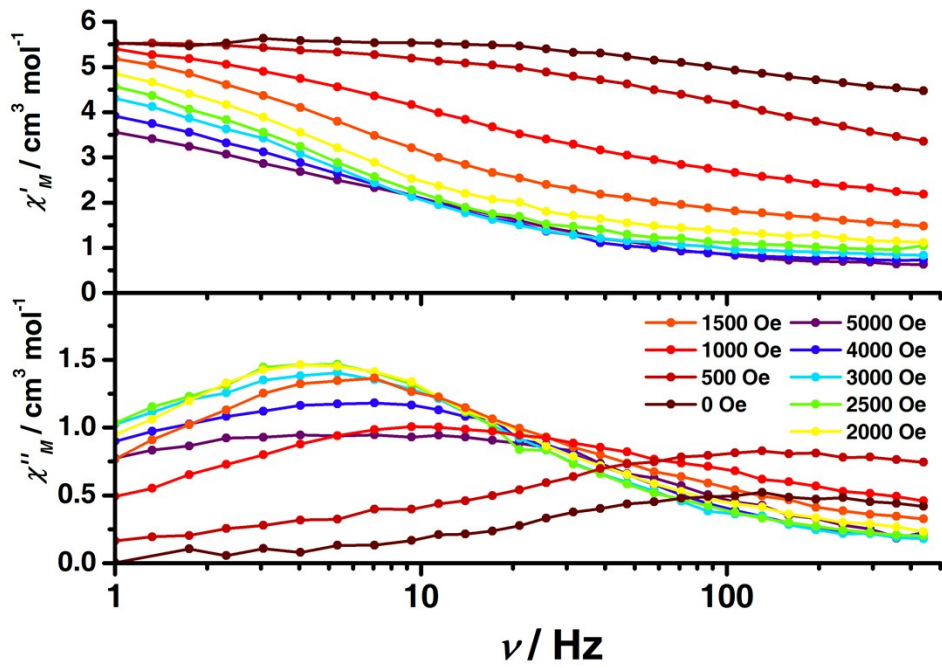


**Figure S4.** Field dependence of in-phase ( $\chi_M'$ ) and out-of-phase ( $\chi_M''$ ) susceptibilities at 4 K under different fields for **1**. The solid lines are guides to the eyes.

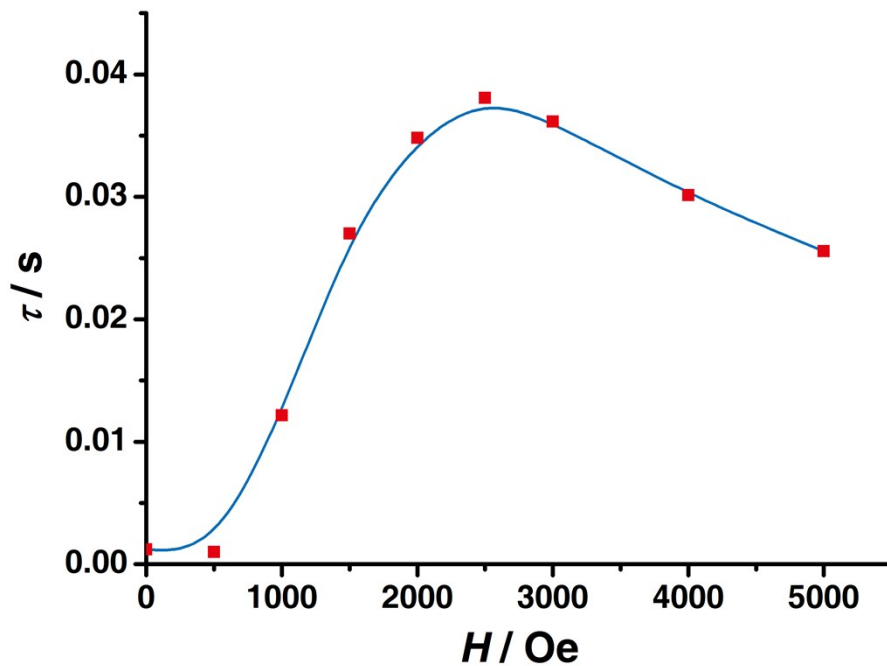


**Figure S5.** Field dependence of the relaxation time at 4 K for **1**. The solid line is a guide for the eyes.

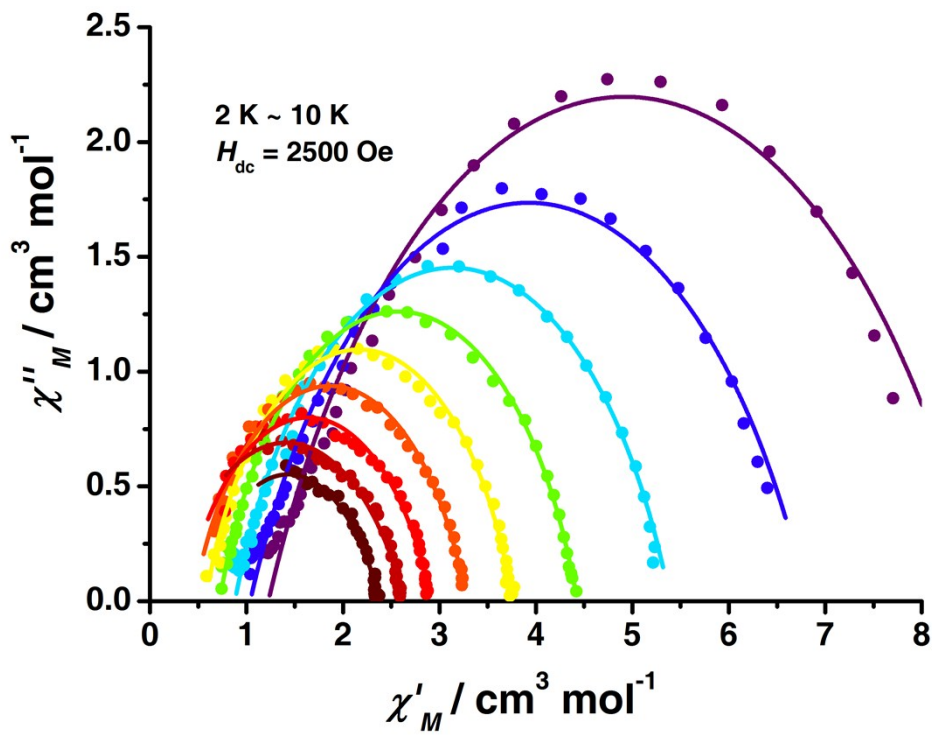


**Figure S6.** Cole–Cole plot for **1** under an applied field of 2500 Oe. The solid lines are the best fits to the experimental data.

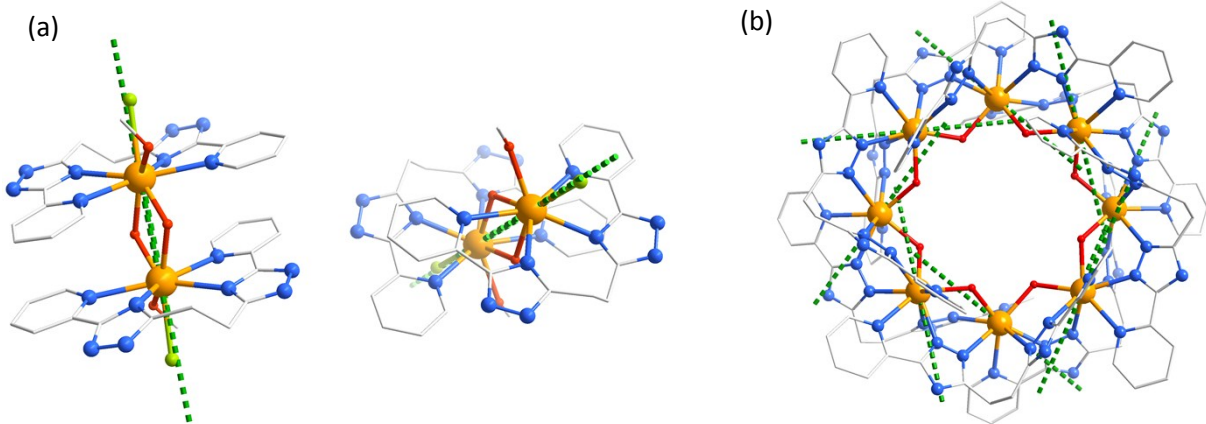


**Figure S7.** The calculated orientations of the ground-state magnetic anisotropy of each local Dy(III) ion for **1** and **2**.